SLAC-PUB-11673
hep-ex/0601020

ISR PHYSICS AT BABAR

V.Druzhinin [a]
Representing the BaBar Collaboration
Budker Institute of Nuclear Physics, 630090 Novosibirsk, Russia

Abstract. We present a review of BaBar results on e+e- annihilations into exclusive hadronic final states using the initial state radiation technique. Cross sections over the $\sqrt{s}$ range from threshold to 4.5 GeV, with very small point-to-point systematic errors, are presented for the 3π, $2(\pi^+\pi^-)$, $3(\pi^+\pi^-)$, $2(\pi^+\pi^-)2\pi^0$, $K^+K^-\pi^+\pi^-$, $2(K^+K^-)$ and $p\bar{p}$ final states. The proton form factor and the ratio of its electric and magnetic components are also presented.

1 Introduction

The BABAR detector [1] collect data at the PEP-II asymmetric-energy e^+e^- collider where 9-GeV electrons collide with 3.1-GeV positrons. The detector covers about 85% of the solid angle in the e^+e^- center-of-mass (c.m.) frame and provides excellent charged particles tracking and identification, and photon detection.

These detector features and high luminosity collected at the PEP-II allow to study the processes of e^+e^- annihilation into different hadronic states using initial state radiation (ISR) technique. In the ISR processes, $e^+e^- \to \gamma X$, a photon of energy E_γ is emitted by the initial electron or positron. As result the produced hadronic system has invariant mass $m = \sqrt{s(1-x)}$, where $\sqrt{s}$ is e^+e^- c.m. energy and $x = 2E_\gamma/\sqrt{s}$. The mass spectrum of the hadronic system X is related to the $e^+e^- \to X$ cross section as

$$\frac{d^2\sigma(e^+e^- \to \gamma X)}{dx\, d\cos\theta_\gamma} = W(s, x, \theta_\gamma)\sigma(m). \qquad (1)$$

Here W is well-known photon radiator function describing ISR photon energy and angular distribution. The ISR photon is emitted predominantly along electron or positron direction. In our approach with detection of the ISR photon at large angle we use only about 10% of ISR events.

2 Selection of ISR events and background subtraction

For analysis we select events with all final particles (including hard ISR photon) detected. The charged particle identification is used to recognize the specific hadronic state and suppress background. For selected events we perform the kinematic fit with the requirement of energy and momentum balance. The two-photon mass for π^0 candidates is constrained to π^0 nominal mass. The cut on χ^2 of the kinematic fit provides additional background suppression.

[a] e-mail: druzhinin@inp.nsk.su

Contributed to 12th Lomonosov Conference on Elementary Particle Physics,
25-31 August 2005, Moscow, Russia

Work supported in part by Department of Energy contract DE-AC02-76SF00515

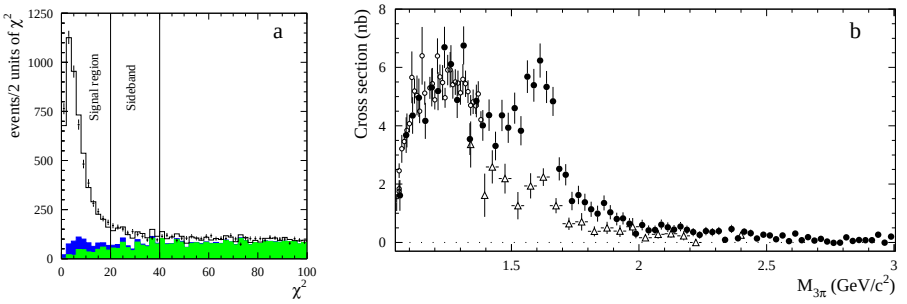

Figure 1: a). The χ^2_p distribution for selected $3\pi\gamma$ candidates for data (points with error bars) and simulation (histogram). The dark and lightly shaded histograms shows the distributions for $e^+e^- \to \pi^+\pi^-\pi^0\pi^0$ and other background processes, respectively. b). The $e^+e^- \to \pi^+\pi^-\pi^0$ cross section measured by BABAR (filled circles), by SND (open circles), and DM2 (open triangles).

The main sources of remaining background are the ISR events with misidentified particles ($K^+K^-\pi^0\gamma$ for $3\pi\gamma$ process, $K^+K^-\gamma$ and $\pi^+\pi^-\gamma$ for $p\bar{p}\gamma$), events with high-energy π^0 instead of ISR photon ($p\bar{p}\pi^0$ for $p\bar{p}\gamma$). The third class of background processes is all other ISR processes and processes of continuum annihilation into quark-antiquark. For example, the χ^2 distribution for $e^+e^- \to \gamma\pi^+\pi^-\pi^0$ candidates is shown in Fig. 1a and seen to be well described by our simulation. Backgrounds from ISR events with misidentified particles ($K^+K^-\pi^0\gamma$) and events with a high-energy π^0 mimicing an ISR photon ($\pi^+\pi^-\pi^0\pi^0$) also peak at low chi^2 values (dark shaded histogram in Fig. 1a), but are a small fraction of the signal, and are measured from the data as a function of 3π mass and subtracted. Other sources of background involve missing or spurious particles and give a broad χ^2 distribution (light shaded histogram); they are subtracted using the χ^2 sideband region indicated.

3 Results

The $\pi^+\pi^-\pi^0$ final state [2]. The $e^+e^- \to 3\pi$ is a key process for study of the excited ω states. The measured $e^+e^- \to 3\pi$ cross section for the mass above 1.05 GeV is shown in Fig. 1b. Our results are consistent with data obtained by SND collaboration for energies below 1.4 GeV, but significantly exceed previous DM2 results for the mass region of ω'' resonance. From the fit of the cross section by a sum of the contributions of ω, ϕ, ω', and ω'' mesons we obtained the parameters of excited ω states: $M_{\omega'} = 1350 \pm 30$ GeV/c^2, $\Gamma_{\omega'} = 450 \pm 100$ GeV/c^2, $M_{\omega''} = 1660 \pm 10$ GeV/c^2, $\Gamma_{\omega''} = 230 \pm 40$ GeV/c^2.

The $\pi^+\pi^-\pi^+\pi^-$, $\pi^+\pi^-K^+K^-$, $K^+K^-K^+K^-$ final states [3]. Our results on the measurement of the cross sections of e^+e^- annihilation into four

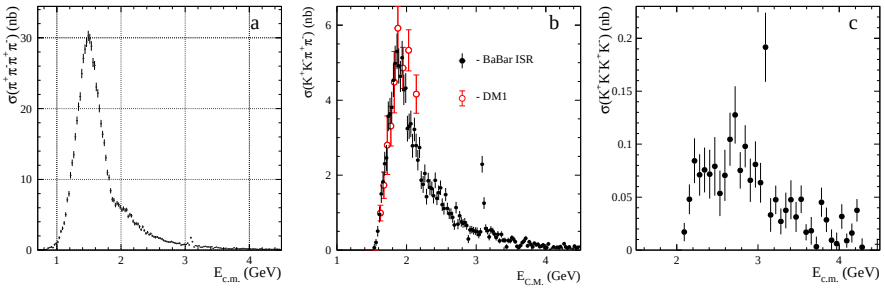

Figure 2: The measured cross sections for $e^+e^- \to \pi^+\pi^-\pi^+\pi^-$ (a), $e^+e^- \to \pi^+\pi^- K^+K^-$ (b), $e^+e^- \to K^+K^-K^+K^-$ (c).

charged particles are shown in Fig.2. This $e^+e^- \to \pi^+\pi^-\pi^+\pi^-$ process (Fig.2a) has large cross section, and its accurate measurement is important for calculation of the hadronic contribution into $(g-2)$ of muon. The BABAR data are in good agreement with previous direct e^+e^- measurements. For energies above 1.4 GeV they have world's best accuracy. From analysis of the 3-pion and 2-pion mass distributions we conclude that dominant intermediate state in this process is $a_1(1260)\pi$. For energies above 2 GeV the $f_0(1370)\rho$ intermediate state is also seen.

The cross section for $e^+e^- \to K^+K^-\pi^+\pi^-$ is shown in Fig. 2b. This process proceeds via $K^*K\pi$, $\phi\pi\pi$, and ρKK intermediate states. We also present the first measurement of the $e^+e^- \to K^+K^-K^+K^-$ cross section (Fig. 2c).

The $p\bar{p}$ final state [4]. The cross section for $e^+e^- \to p\bar{p}$ depends on two form factors: electric (G_E) and magnetic (G_M). From measuring the total cross section we can extract a combination of form factors. We define the effective form factor as $F(m) = \sqrt{(|G_M(m)|^2 + \tau|G_E(m)|^2)/(1+\tau)}$ where $\tau = 2m_p^2/m^2$. Such definition allows to compare our form-factor results with the data from previous e^+e^- and $p\bar{p}$ experiments which use the assumption that $|G_E| = |G_M|$. The ratio of the form factors can be extracted from the analysis of the distribution of the proton helicity angle (θ_p) in the $p\bar{p}$ rest frame. The ISR approach provides full θ_p coverage and hence high sensitivity to $|G_E/G_M|$. In contrast to previous e^+e^- and $p\bar{p}$ experiments, our measurement of cross section does not use the assumption that $|G_E| = |G_M|$. It should be noted that $p\bar{p}$ mass resolution near the $p\bar{p}$ threshold is less than 1 MeV and comparable with the energy spread of e^+e^- machines.

The $\cos\theta_p$ distribution was fitted in six bins of $m_{p\bar{p}}$ by a sum of two distributions corresponding G_E and G_M terms in the differential cross section. The G_E distribution is close to $\sin^2\theta$, the G_M distribution to $1+\cos^2\theta$. The obtained mass dependence of $|G_E/G_M|$ is shown in Fig. 3a. Our result disagrees significantly with previous measurement from LEAR [5].

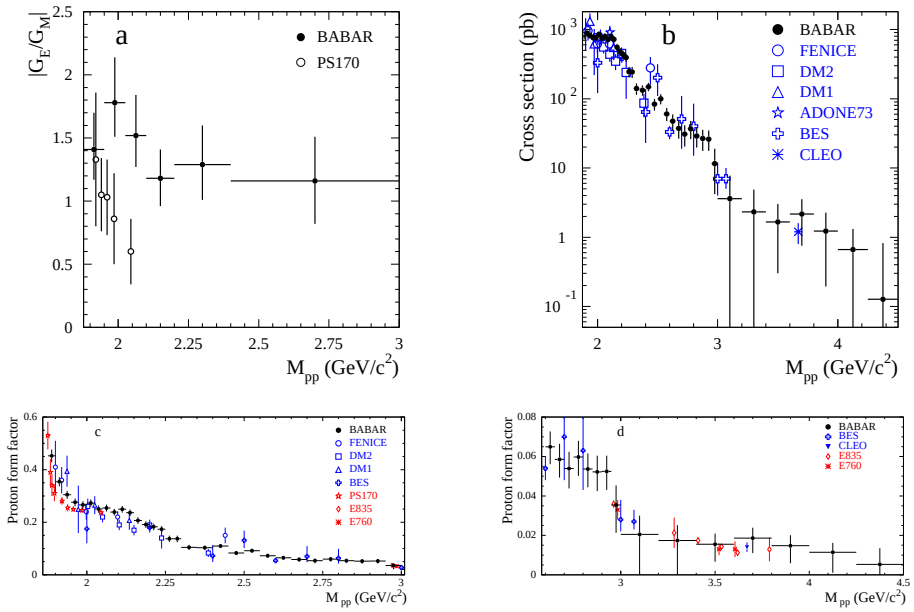

Figure 3: a). Mass dependence of the ratio $|G_E/G_M|$. b). The measured cross sections for $e^+e^- \to p\bar{p}$. c). and d).The effective proton form factor.

The obtained $e^+e^- \to p\bar{p}$ cross section shown in Fig. 3b (the contributions of J/ψ and $\psi(2S)$ decays are subtracted) is in reasonable agreement with previous e^+e^- measurements. Our data more full and accurate for energy range below 3 GeV. The effective form factor is shown in Fig. 3c,d. It has a complex mass dependence. We confirm the near-threshold enhancement in the form factor observed in the LEAR experiment. There are also two mass regions, near 2.25 GeV/c^2 and 3 GeV/c^2, that exhibit steep decreases in the form factor. This unusual mass dependence has never been discussed in the literature.

The 6π final states [6]. The near-threshold enhancement in the $p\bar{p}$ mass spectrum may be a manifestation of $p\bar{p}$ subthreshold resonance. Such resonance may be seen in $e^+e^- \to hadrons$ cross section near 1.9 GeV. A narrow dip in the $e^+e^- \to 6\pi$ cross section was observed in DM2 experiment and in the diffractive photoproduction of six pions in FOCUS experiment [7]. Our results on measurement of six pion cross sections are shown in Fig. 4. In both six-pion cross sections the dips near 1.9 GeV are clearly seen. The cross sections are fitted by a sum of resonance and continuum amplitudes. The fit results the resonant mass 1880 ± 30 MeV/c^2 (1860 ± 20 MeV/c^2) and width 130 ± 30 MeV/c^2 (160 ± 20 MeV/c^2) for $3(\pi^+\pi^-)$ ($2(\pi^+\pi^-)2\pi^0$) mode. The obtained width is significantly differ from the FOCUS result of 29 ± 14 MeV/c^2.

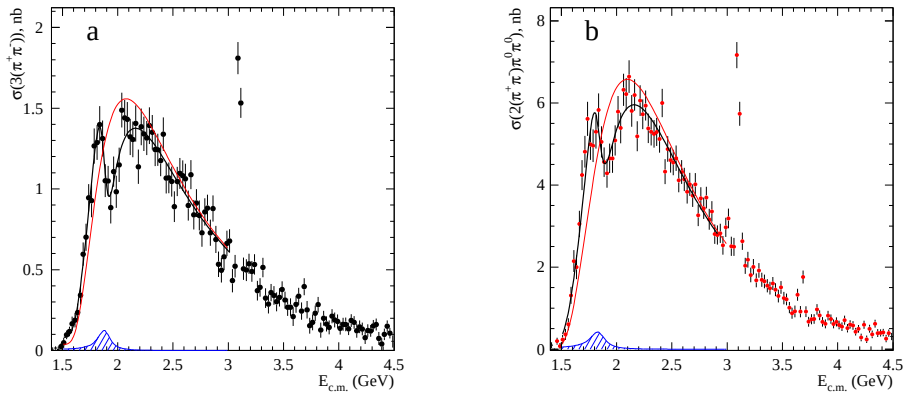

Figure 4: The measured cross sections for $e^+e^- \to 3(\pi^+\pi^-)$ (a), $e^+e^- \to 2(\pi^+\pi^-\pi^0)$ (b).

4 Summary

The program to measure low-energy hadronic cross sections using ISR is well underway at BaBar. We have presented the cross section measurements for $e^+e^- \to \pi^+\pi^-\pi^0$, $2(\pi^+\pi^-)$, $K^+K^-\pi^+\pi^-$, $2(K^+K^-)$, 6π. We significanly improved accuracy for these cross sections in the 1.4–4.5 GeV energy range.

We have also measured $e^+e^- \to p\bar{p}$ cross section and extracted the proton effective form factor. These are most full and accurate $e^+e^- \to p\bar{p}$ data in the energy range from the threshold up to 3 GeV. In contrast to previous experiment, our measurement does not use the assumption that $|G_E| = |G_M|$. From analysys of the proton angular distribution we have extracted the energy dependence of the $|G_E/G_M|$ ratio. Its value is found to be significanly greater than unity for energies below 2.1 GeV.

The analysys of $\pi^+\pi^-$, K^+K^-, $K\bar{K}\pi$, $\pi^+\pi^-\pi^0\pi^0$, 5π, and $D^{(*)}\bar{D}^{(*)}$ final states are in progress at BaBar.

References

[1] B.Aubert *et al.*, *Nucl. Instr. and Meth.* **A** 479, 1 (2002).
[2] B.Aubert *et al.*, *Phys.Rev.* **D** 70, 072004 (2004).
[3] B.Aubert *et al.*, *Phys.Rev.* **D** 71, 052001 (2005).
[4] B.Aubert *et al.*, hep-ex/0512023, *accepted by Phys.Rev.* **D**.
[5] G. Bardin *et al.*, *Nucl. Phys.* **B** 411, 3 (1994).
[6] B.Aubert *et al.*, *submitted to Phys.Rev.* **D**.
[7] P.L. Frabetti *et al.*, *Phys. Lett.* **B** 514, 240 (2001).